DOI: 10.1021/ma100137w

Macromolecules
ARTICLE

Subglass Cooperative Mechanical Relaxations and Activation Entropy in Heterocyclic Polymer Networks

Antonio Bartolotta,[†] Giovanni Carini, Jr.,[‡] Giuseppe Carini,*[,‡] Gaetano Di Marco,[†] and Gaspare Tripodo[‡]

[†]*Istituto per i Processi Chimico-Fisici del C. N. R., Sez. di Messina, Viale F. Stagno D'Alcontres, I-98166 Messina, Italy, and* [‡]*Dipartimento di Fisica, Universita' di Messina, Viale F. Stagno D'Alcontres 31, I-98166 Messina, Italy*

Received January 19, 2010; Revised Manuscript Received April 7, 2010

ABSTRACT: Measurements of differential scanning calorimetry, dynamic mechanical analysis, and dilatometry have been performed in heterocyclic polymer networks (HPNs), whose effective network density has been gradually varied keeping the overall chemical structure essentially unchanged. Evidence of a growing intermolecular cooperativity for a local relaxation motion is offered by the investigation of the subglass mechanical β-relaxation, whose frequency factor and apparent activation energy strongly increase with increasing cross-linking density from about 10^{15} s^{-1} and 44.2 kJ/mol to about 10^{19} s^{-1} and 69.8 kJ/mol. The analysis of the characteristics of the mechanical β-relaxation suggests the existence of cooperative transitions of consecutive relaxing units, mainly driven by the crank-shaft motion of the network junctions between the isocyanurate heterocycles building up the structure. Comparison with previous results concerning the dielectric β-relaxation evidence a less cooperative character and a different microscopic origin for the conformational transitions driving the dielectric process. Moreover, a decrease in the thermodynamic fragility with increasing network density has been revealed, which contrasts with the increasing dynamic fragility, as measured by dielectric and mechanical probes.

Introduction

Polymers show anelastic relaxations in the glassy state, which are due to local conformational transitions of some groups building up the main chain. In most cases, the relaxations and the related anomalies in the mechanical spectra are broader than those arising from a single relaxation time as a consequence of random deviations in the local arrangements of the relaxors. These types of motions are thermally activated and induce relaxational losses as well as associated dispersions in the mechanical behaviors of polymers. The local conformational motion of chain groups is a consequence of residual degrees of freedom, sometimes associated with a residual excess volume that is available to perform changes of conformation. As a rule, subglass relaxations can be distinguished as simple and complex depending on their respective degree of cooperativity.[1] Simple relaxations are characterized by usual characteristic frequencies ω_0, near 10^{13} s^{-1} in an Arrhenius plot, which imply small or negligible variations of the activation entropy associated with the specific local motion. Quite differently, complex relaxations exhibit large characteristic frequencies associated with a significant activation entropy, which can be related to a high degree of intra- or intermolecular cooperativity between the local relaxors.[1,2]

To explore the puzzling aspect of complexity concerning the secondary relaxations, we have performed a study of dynamic mechanical analysis in model polymer systems where the density of cross-links between the molecular units can be changed without altering the chemical structure. In a class of heterocyclic polymer networks (HPNs) based on isocyanurate rings,[3,4] in fact, it is possible to change the ratio of bifunctional to monofunctional monomers in the reaction mixture giving rise to systematic changes of the effective network density and keeping their overall chemical structure essentially unchanged. The gradual variation of the cross-link density is expected to enhance the degree of intermolecular cooperativity between the locally mobile molecular units, resulting in a progressive and substantial increase in the activation entropy. In fact, increasing values of the characteristic frequency, ω_0, and the apparent activation energy, E_{act}, characterizing the subglass mechanical β-relaxation have been observed with increasing network density. This increase has been associated with an activation entropy marking the growing cooperative character of the underlying conformational motion of the relaxing molecular groups.

A further important subject in amorphous polymers concerns their classification in the context of "fragility", a concept introduced by Angell[5−7] to classify glass-forming liquids according to their cooperative relaxation dynamics through the glass-transition region. In particular, contrasting behaviors have been observed for the "thermodynamic" and "dynamic" fragility of polymers, and doubts have been raised about the extension of the strong/fragile classification scheme to these systems.[8,9] The relation between thermodynamic fragility, given by the change in heat capacity at the glass-transition temperature, T_g, and the dynamic fragility, determined by dielectric and mechanical experiments probing the structural rearrangements of glass-forming liquids when T_g is approached, has been explored in HPNs showing that an increasing network density depresses the former while enhancing the latter.

Experimental Details

HPNs were obtained by simultaneous trimerization reaction of 1,6-hexamethylene diisocyanate (HDI), hexyl isocyanate (HI), and hexabutyl distannum oxide (HBDSO, catalyst) purchased

*Corresponding author. E-mail: carini@unime.it.

 Published on Web 04/21/2010

from Aldrich Co. and used as received. The method of HPN synthesis, described elsewhere,[3] produced a regularly cross-linked copolymer with controlled molar fractions of two-arm (linear, L) and three-arm (cross-linked, N) segments, whose chemical schemes are shown in Figure 1. Table 1 reports some structural parameters concerning HPNs and evaluated by assuming a full conversion of the reacting groups: L/N refers to relative ratio between linear and network structure, $< M_R >$ is the molecular weight of the monomer unit, and $< M_c >$ is the mean molar mass of chain strands between network junctions. In the following, the acronyms L100, L60, L43, and L0 will be used to indicate the ratios L/N = 100/0, 60/40, 43/57 and 0/100, respectively, the latter concentration referring to a wholly cross-linked structure or a full network. To avoid undesirable effects due to contamination from absorbed water moisture, the samples were dried at room temperature under vacuum of 10^{-4} mbar for ~12 h before each run of measurements and then analyzed by maintaining the experimental chamber under a controlled atmosphere of nitrogen. Dynamic mechanical thermal properties (storage modulus E' and loss modulus E'') were investigated in tensile mode between 120 and 450 K at heating rate of 1 K/min using a dynamic mechanical thermal analyzer (DMTA) from Polymer Laboratories. The frequency interval ranges between 0.3 and 30 Hz.

The glass-transition temperatures, T_g, were determined over the temperature interval between 220 and 450 K by thermograms performed with a heating rate of 20 K/min by a Perkin-Elmer Pyris1 differential scanning calorimeter (DSC) calibrated with indium and zinc standards. The specific heat capacities, C_p, were determined using a standard sapphire sample as a reference.

Thermal expansion measurements were made from 100 to 350 K using a Netzsch Industries silica pushrod LVDT horizontal dilatometer with a heating rate of 2 K/min.

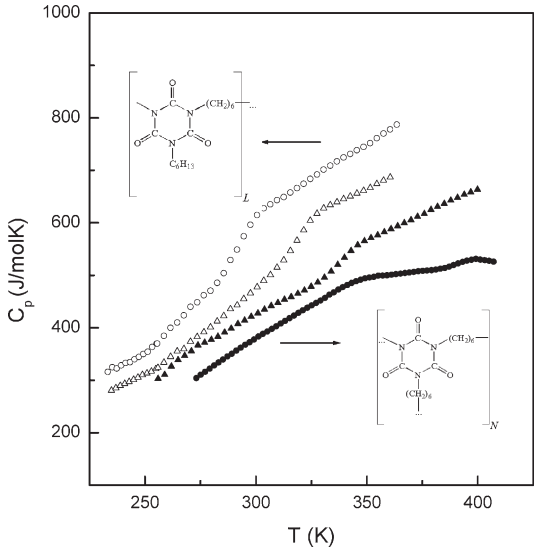

Figure 1. Temperature dependences of heat capacities through the glass-transition region for HPN: (○), L100; (△), L60; (▲), L43; (●), L0. The generalized chemical schemes of linear (L100) and fully cross-linked (L0) heterocyclic polymer networks are also included.

Results

A. Thermal Transitions. Sudden C_p jumps in the glass-transition intervals are observed on heating HPNs above 220 K (Figure 1). Step-like features are also observed in all of the samples around 270 K, whose nature is at present unclear. Further exploration of such samples is in progress to analyze thoroughly these small humps, whose possible origin, however, has any relevance for the discussion concerning the fragility of HPN. The complete absence of melting endotherms in this temperature interval and the increase in T_g from 291 K for L100 to 318 K for L60 and 335 K for L43 and to 392 K for L0 indicate that the HPNs can be regarded as homogeneous amorphous systems. Increasing network or cross-link density shifts the glass transition to higher temperatures and reduces the change in the heat capacity ΔC_p ($= C_{p,l} - C_{p,g}$) at T_g, where $C_{p,l}$ and $C_{p,g}$ represent the heat capacities evaluated in the liquid and glassy states, respectively. In the context of "fragility" proposed by Angell,[5] the changes in the heat capacity at T_g define the "thermodynamic" fragility. It is usually assessed by ΔC_p or by the ratio $C_{p,l}/C_{p,g}$, fragile glass-formers exhibiting large changes in the heat capacity at T_g as opposite to small variations characterizing strong systems.

B. Mechanical Transitions. To better illustrate the effects of cross-linking density on the relaxation dynamics of HPNs, the experimental results for the loss tangent tan δ

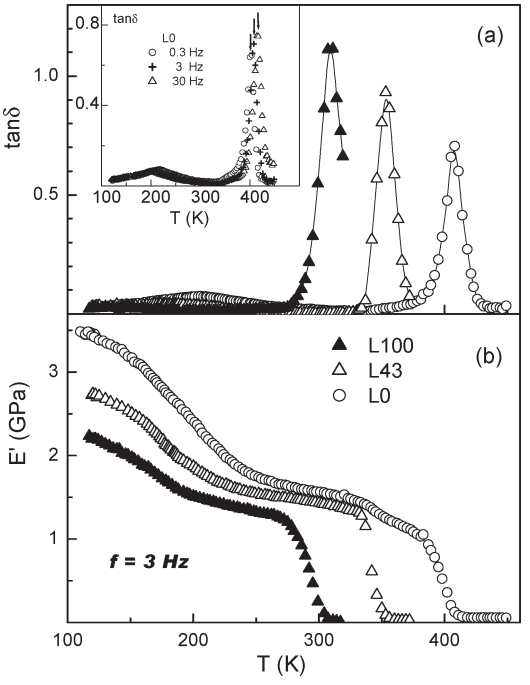

Figure 2. Temperature dependences of (a) the loss tangent tan δ and (b) the tension dynamic modulus E' in HPNs at a frequency of 3 Hz: L100 (▲); L43 (△); L0 (○). The continuous lines are only guides for eyes. The inset shows the effect of driving frequency on the temperature dependence of tan δ in L0.

Table 1. Parameters of the Studied HPNs Having a Relative Ratio L/N of Linear to Network Content[a]

L/N	ρ (kg/m^3)	T_g (K)	$< M_c >_{theor}$ (g/mol)	$< M_R >$ (g/mol)	E_{act} (kJ/mol)	τ_0^{-1} (s^{-1})
100/0	1148	291	∞	295	44.2	4.93×10^{15}
60/40	1188	318	695	278		
43/57	1200	335	473	270	56.0	2.14×10^{18}
0/100	1238	392	252	252	69.8	3.68×10^{19}

[a] ρ is the density at room temperature, T_g is the glass-transition temperature, $< M_c >$ is the average molecular weight between cross-links, and $< M_R >$ is the molecular weight of monomers. The values of the apparent activation energy, E_{act}, and the characteristic frequency, τ_0^{-1}, have been determined by the Arrhenius plot of Figure 4.

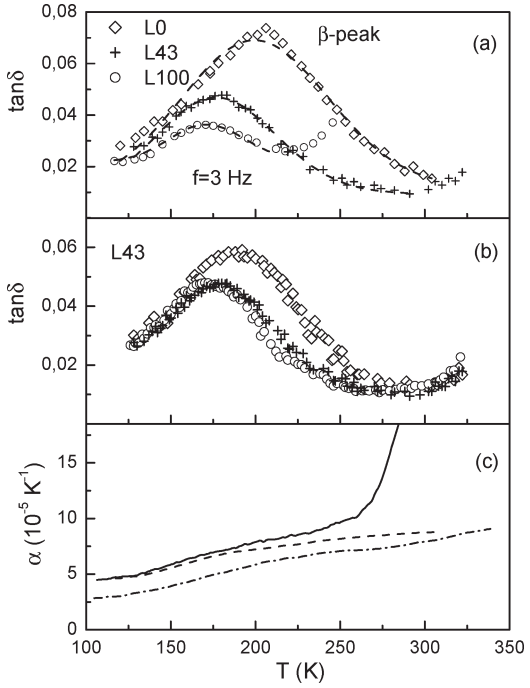

Figure 3. (a) Comparison of the β-relaxation losses in HPNs at a frequency of 3 Hz: L100 (○); L43 (+); L0, (◇); dashed lines represent the fitting curves obtained by eq 2. (b) Low temperature tan δ of L43 at selected frequencies: 0.3 (○), 3 (+), and 30 Hz (◇). (c) Temperature dependence of the thermal expansion coefficient in HPNs: L100, solid line; L43, dashed line; L0, dashed-dotted line.

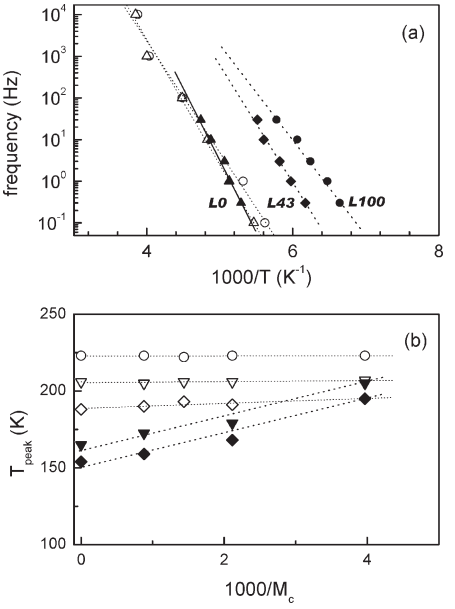

Figure 4. (a) Arrhenius plots of the mechanical (solid symbols) and dielectric (open symbols) β-loss peaks for HPNs: L100 (●); L43 (◆); L0 (▲). The temperatures, T_{peak}, of the β-peak maxima have been taken from $E''(T)$ curves; the dielectric data are from $\varepsilon''(T)$ behaviors reported in ref 4. (b) Peak temperatures of mechanical (solid symbols) and dielectric (open symbols) β-relaxations for HPNs as a function of $1/M_c$ at selected frequencies: 1 (◆), 10 (▼) and 100 Hz (○).

(= $E''(T)/E'(T)$, where E'' and E' represent the loss and storage moduli, respectively) at a mechanical frequency of 3 Hz for the samples L100, L43 and L0 are compared in Figure 2a. As the temperature is increased from 120 K, tan δ exhibits the β-relaxation peak, and above 250 K, it exhibits the large α-relaxation peak typical of the glas-to-rubber transition. The modulus E' exhibits a significant inflection in the same temperature region where the β-peak is observed, Figure 2b. With increasing temperature above this region, a linear decrease in E', followed by sharp drops of about two orders of magnitude, is observed, which mark the large softening of the system associated with the cooperative segmental motion at the glass transition. With increasing network density, the α-loss peak moves to higher temperatures and exhibits a decreasing strength, as weighed by the magnitude of the loss peak, the latter feature being in clear contrast with the behavior observed for the β-relaxation (Figure 3a). The α-loss peaks shift to higher temperatures as the mechanical driving frequency is increased (inset of Figure 2a).

As the temperature is increased from 120 to 250 K, the mechanical loss of HPNs is mainly regulated by the β-relaxation, whose contribution to tan δ is depicted by using a more expanded scale in Figure 3. The strength and the temperature of β-loss peak increase with increasing network density (Figure 3a), the latter shifting from ~167 K in L100 through 179 K in L43 to 210 K in L0 (at 3 Hz). All β-loss peaks shift to higher temperatures as the mechanical driving frequency is increased (Figure 3b), as a clear indication of the thermally activated nature of the underlying process. Over the same temperature range, the storage modulus, E', (Figure 2b) exhibits corresponding inflections, which evidence the same characteristics described above for the β-loss peaks. These observations indicate that cross-linking has a strong impact on β-relaxation strength, which is enhanced by more than a factor of 2 by going from the apparently linear heterocyclic polymer (L100) to the wholly cross-linked HPN (L0).

The explored frequency range enables us to evaluate the apparent activation energy, E_{act}, and the characteristic frequency, τ_0^{-1}, of the β-relaxation process. The Arrhenius plot of the frequencies versus the reciprocal temperatures of the mechanical loss maxima is shown in Figure 4a and gives the values of E_{act} and τ_0^{-1} reported in Table 1. Because the peaks in tan δ can be significantly shifted because of difference in the value of $E'(T)$,[10] the temperatures T_{peak}, of the β-peak maxima have been taken from $E''(T)$ curves. This allows us for a more consistent comparison with the results of previous dielectric measurements on the same polymers,[4] which are also included in the same Figure. The latter disclosed values of the activation energy associated with the dielectric β-relaxation ranging in the most restricted interval between 50.4 (L100) and 58.3 kJ/mol (L0). It is worth noting that the frequency factors exhibit unusually large values that vary from $\sim 10^{15}$ (L100) to 10^{19} s^{-1} (L0), the interval of variation resulting, also, in this case, much more wide than that assessed by dielectric measurements (from 3.4×10^{15} (L100) to 2.9×10^{16} s^{-1} (L0)[4]). As it will be explained and extensively discussed in the following, the discrepancy between mechanical and dielectric data probably takes its origin from different kinds of local molecular motion probed by the two techniques.

Discussion

A. Mechanical Subglass Relaxations. The relaxation dynamics of these HPNs, governed by single α- and β-relaxations, suggests that the chain connectivity enhanced by cross-linking gives rise to single phase networks with a high degree of homogeneity and isotropic properties. Now, the mechanical, such as the dielectric, spectroscopy probes the relaxation processes that impose their length scales in the experiment. The relevant length scale (i.e., the size of the relaxing

molecular groups involved) for the β-relaxation is clearly of local nature, implying that both of the probes are sensitive to local motion within the polymer network.

Figure 4b shows the temperatures, T_{peak}, of the β-peak maxima revealed in $\varepsilon''(T)$ and $E''(T)$ over the 1−100 Hz frequency range by dielectric[4] and mechanical probes as a function of the inverse of M_c, that is, with increasing network density. Dielectric and mechanical T_{peak} values exhibit different behaviors: the dielectric T_{peak} remains essentially invariant, whereas a variation of ~40 K is observed for the mechanical T_{peak} by going from the linear (L100) to the cross-linked HPN (L0). The different network density dependence of β-relaxations can be considered to be a strong indication of the fact that dielectric and mechanical spectroscopy probe different, even if correlated, kinds of local motion. The coupling between dielectrically and mechanically active motions is proved by comparable time scales, activation energies (Table 1; Table 4 of ref 4), and similar behaviors of the relaxation strength with increasing network density.

Dielectric spectroscopy (DS) tests the motion of dielectrically active dipoles, the polar NCO or isocyanurate heterocycle (ISH) rings, whose concentration changes slightly by increasing network density.[4] It has been suggested that conformational transitions of ISHs, distributed in loosely packed regions of the polymer network, drive the dielectric β-relaxation. The fraction of these regions is believed to increase markedly by going from the densely packed structure of L100, based on linear chains of two-arm ISHs, to the loosely packed network of L0 mainly built on three-arm ISHs, giving rise to the observed large enhancement of the β-relaxation strength. Following the structural similarity between isocyanurate and cyclohexyl rings, the conformational motion of ISHs is assumed to be like the "chair−boat−chair" transitions of cyclohexyl rings.[4] Now, it has been shown that the local motion of cyclohexyl rings is independent of the local intermolecular packing:[11] mixtures of polycyclohexylmethacrylate (PCHMA) and an additive (pentachlorobiphenyl) do not reveal the suppression of the β-relaxation, this effect being usually due to a remarkable sensitivity of the molecular rearrangements to the local volume fluctuations. This means that the discussed variation in the local packing of HPNs cannot be considered to be causing the increase in the β-relaxation strength. Moreover, the density of HPNs (see Table 1) shows a well definite increase with increasing cross-linking. Following these considerations, we will examine more exhaustively the dielectric and mechanical results concerning the subglass relaxation process in HPNs to suggest a molecular motion mechanism accounting for the differences revealed by the two probes. It is worth noting that the mechanical β-relaxation is associated with a pronounced increase in the thermal expansion, α_{th}, which is smeared out over the same temperature interval (Figure 3c). The existence of a distinct correlation between subglass relaxations and a sudden variation of α_{th} implies that the conformational transitions driving the mechanical β-relaxation require a relevant fraction of swept-out volume. This observation strongly supports the collective crank-shaft motion of several segments within the C_6H_{13} nonbridging groups and the $(CH_2)_6$ arms linking the ISHs as possible a origin for the relaxation.[12−15] The value of 44.2 kJ/mol determined for the apparent E_{act} in L100, the linear HPN, is slightly higher but quite close to the value of 39 kJ/mol characterizing the crank-shaft motion in the linear high density polyethylene (HDPE).[15] Possible motivation for this difference is that the highly polar ISH rings, whose local motions in L100 originate the dielectric β-relaxation at a higher temperature than the mechanical one (Figure 4b), give rise to substantial interchain interactions, and impose mechanical constraints on the crankshaft segments. This is demonstrated by the increase in E_{act} with increasing cross-linking from 44.2 kJ mol^{-1} in L100 to 69.8 kJ mol^{-1} in L0. The low value of E_{act} observed in L100 accounts for the crankshaft motions of two $(CH_2)_6$ bridging arms and one C_6H_{13} nonbridging group, the conformational transitions of the latter being surely characterized by smaller potential barriers. By increasing network density, all side groups are increasingly transformed in bridging arms between the polar rings and experience constraints that rise the potential barriers between the conformations explored by the crankshaft motion.

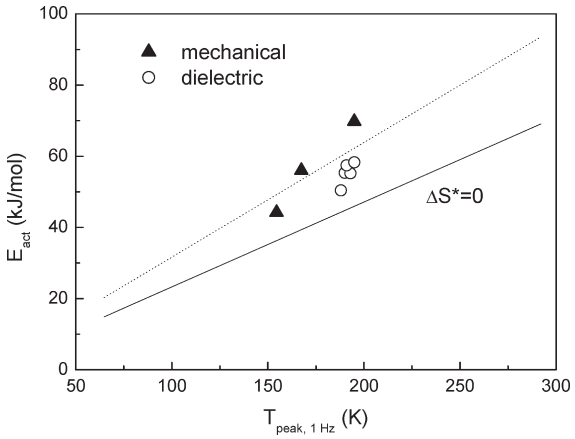

Figure 5. Apparent activation energies, E_{act}, versus the peak temperatures, $T_{peak,1}$, of dielectric (○) and mechanical (▲) β-relaxation at 1 Hz. The behaviors given by eq 1 for $\Delta S^* = 0$ (the noncooperative limit) and $\Delta S^* = 83.68$ J/Kmol are reported as solid and dotted lines, respectively.

The crank-shaft motion of $(CH_2)_6$ arms linking the ISHs exhibit the characteristics of an intermolecularly cooperative relaxation. The unusually high values of the frequency factor (Table 1) do not fit Starkweather's definition of "simple" relaxations with zero activation entropy.[1] They point to the existence of a "complexity" of the relaxation process, which involves cooperative motion of neighboring molecules. The main point is that all samples exhibit β-loss peaks that are unexplainable in terms of a single relaxation time. The existence of a distribution of relaxation times for the β-process observed in HPN implies a distribution of activation energies, activation entropies, or both and complicates the analysis of the experimental data. Tentatively, the Eyring's equation from the theory of absolute reaction rate

$$f = \frac{kT}{2\pi h} e^{-\Delta H^*/RT} e^{\Delta S^*/R}$$

has been applied to relate the apparent activation energies, E_{act}, determined by the Arrhenius plots to the activation enthalpy, ΔH^*, of the relaxation process. In the equation above, ΔS^*, the activation entropy and the other symbols have the usual meaning. The relationship between E_{act} and ΔH^*, $E_{act} = \Delta H^* + RT$, can be rearranged to derive the following equation, which links E_{act} and the temperature, $T_{peak,1}$, of the mechanical loss maxima at $f = 1$ Hz[1]

$$E_{act} = RT_{peak,1}\left[1 + \ln\left(\frac{k_B T_{peak,1}}{2\pi h}\right)\right] + T_{peak,1}\Delta S^* \quad (1)$$

The plot of E_{act} versus $T_{peak,1}$ reported in Figure 5 reveals increasingly higher values by going from L100 to L0, which

Table 2. Values of the Parameters E_m, E_0, τ_0^{-1}, and $N\gamma^2$ for the β-relaxation in HPNs[a]

L/N	E' (GPa)	τ_0^{-1} (s^{-1})	E_m (kJ/mol)	E_0 (kJ/mol)	$N\gamma^2$ (10^{-12} J^2 m^{-3})	γ (eV)
100/0	1.78	6.0×10^{14}	44.3	5.4	1.60	0.12
43/57	2.28	7.3×10^{16}	52.9	10.3	9.68	0.29
0/100	2.87	5.1×10^{18}	66.7	14.2	25.26	0.47

[a] Values of the storage modulus, E', are taken at 200 K.

are paralleled by a well definite increase in the activation entropy, ΔS^*, from ~53.6 to 123.5 J/Kmol. Data obtained from dielectric measurements[4] are also included in the same plot: they exhibit a more narrow range of variation with increasing cross-linking in the network, showing activation entropies that range from 34 J/Kmol for L100 to 64.6 J/Kmol for L0. These results imply a growing cooperative character of both the mechanical and dielectric β-relaxations with increasing network density, a larger degree of cooperativity being associated with the local motion explored by the mechanical probe. A possible explanation is that the motion of the conformers, that is, the units of $(CH_2)_6$ arms experiencing the crankshaft conformational change, extends its correlation range from two (in L100) to three arms (in L0) following the conversion of the linear segments in fully cross-linked units, whereas the dielectric response is limited to the motion of ISH rings, whose moves become severely affected by the enhanced long-range segmental motion of the arms.

The above considerations about the mechanical β-relaxation emphasize the existence of a significant degree of cooperativity characterizing the underlying local motion. Therefore, its description in terms of a parallel relaxation, that is, an independent site model, could be not appropriate to investigate the microscopic mechanisms regulating this kind of local motion fully. In the following, however, we will assume a localized site model as a useful first approximation to estimate the relaxation strengths and to perform a comparison between them. The symmetric double-well potential (SDWP) model schematizes the locally mobile relaxing particles in terms of SDWPs having a broad distribution of the barrier height, E, which accounts for random variations in the local environments of particles due to the topological disorder. The relaxation loss is given by[16,17]

$$\tan\delta = \frac{A}{T}\int \exp\left(-\frac{(E-E_m)^2}{2E_o^2}\right) \times \frac{\omega\tau(E)}{1+\omega^2\tau^2(E)}\,dE \quad (2)$$

where

$$A = \frac{N\gamma^2}{4E'k_B\sqrt{2\pi}E_o} \quad (3)$$

The relaxation time, τ, is given by the usual Arrhenius expression, $\tau = \tau_0 e^{E/k_B T}$. E_m and E_0 represent the most probable activation energy and the width of the distribution, N is the number of relaxing molecular groups, γ is an average deformation potential describing the coupling between the mechanical stress and the relaxing centers, E' is the storage modulus, and the other symbols have the usual meanings. Numerical evaluation of the experimental curves by eq 2 gave the values for the relaxation parameters reported in Table 2 and the curves shown by dashed lines in Figure 3. The results show that (i) the values of the mean activation energy, E_m, are in close agreement with those of E_{act} and (ii) both E_m and the product $N\gamma^2$ increase with inclusion of cross-links. The increase in $N\gamma^2$with increasing network connectivity must be mainly determined by the deformation potential, γ, because the number, N, of relaxors, as given in the proposed model by the total concentration of bridging (C_6H_{12}) and nonbridging (C_6H_{13}) arms, decreases only slightly (~5%) by going from the linear (L100) to the fully cross-linked (L0) HPN. Evaluation of the coupling constant, γ, gives the values included in Table 2: γ increases with increasing glass-transition temperature, T_g, disclosing a roughly positive linear correlation. This finding is in agreement with the behaviors generally observed over a wide range of amorphous materials for both of the deformation potentials describing the coupling with longitudinal and transverse sound waves[18,19] and supports the association between the mechanical β-relaxation and the crankshaft motion of both bridging and nonbridging arms of ISH rings. Inclusion of cross-links increases the number of $(CH_2)_6$ bridging arms, which should be characterized by a stronger coupling to the mechanical stress than C_6H_{13} nonbridging groups.

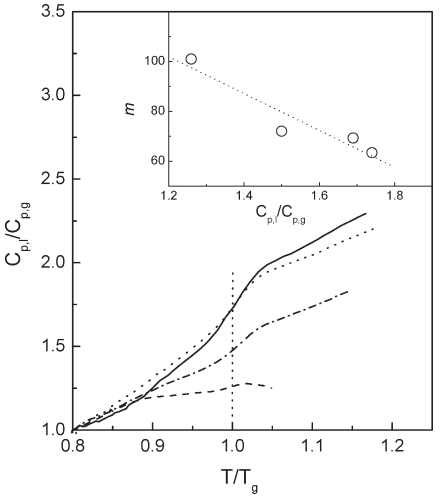

Figure 6. Changes of the heat capacities at T_g, plotted as $C_{p,l}/C_{p,g}$ versus T/T_g, for heterocyclic polymer networks (HPN): L100 (solid line), L60 (dotted line), L43 (dashed-dotted line), and L0 (dashed line). The inset shows the behavior of the dynamic fragility, m, versus the thermodynamic fragility, $C_{p,l}/C_{p,g}$; the dotted line is a guide for eyes only.

B. Thermodynamic versus Dynamic Fragility. The behaviors of $C_{p,l}/C_{p,g}$ versus T/T_g are reported in Figure 6 and reveal a well-defined decrease in the thermodynamic fragility with increasing cross-link density in the network. In particular, the ratio $C_{p,l}/C_{p,g}$ decreases about linearly with decreasing mean molar mass, $< M_c >$, between network junctions. This observation could be discussed in a wider context including the "dynamic" fragility of a glass-forming liquid. The fragility, which has been initially defined by the parameter $m = [(d \log \eta)/(d(T_g/T))]_{T=T_g}$ defining the limiting slope of the viscosity curves at the glass-transition temperature, T_g, permits to place glass-forming liquids in the interval between the two extremes "fragile" and "strong", corresponding to the highest and the lowest value of m, respectively. "Fragile" liquids, such as hydrated $Ca(NO_3)_2$ and *o*-terphenyl, are substances with nondirectional interatomic or intermolecular bonds that permit drastic changes in local

order at the glass transition leading to pronounced deviations from the Arrhenius behavior for the viscosity. By contrast, "strong" liquids (such as SiO_2 or GeO_2), characterized by strong covalent bonds, which preserve the main structural characteristics over broad ranges of temperature, exhibit an Arrhenius dependence of the viscosity. Besides considering the temperature dependence of the viscosity as a manifestation of the fragility, m, the link between different measures of m obtained by various techniques operating in a linear response regime, such as dielectric and mechanical spectroscopy, has also been explored.[6] In this case, the fragility is defined by $m = [(\mathrm{d} \log <\tau>)/(\mathrm{d}(T_g/T))]_{T=T_g}$, where the average relaxation time $<\tau>$ of the primary process is determined by dynamic experiments that probe the structural rearrangements experienced by the glass-forming liquid when the glass-transition temperature, T_g, is approached. The temperature behavior of $<\tau>$ is usually expressed by the Vogel−Fulcher−Tamman (VFT) equation.[20] Within a general context including a wide number of inorganic and organic glass-forming liquids, the values of the "dynamic" fragility, m, given by different techniques appear to agree with each other.[6]

A close relation between dynamic behaviors and thermodynamic properties of glass-forming liquids near the glass transition has been proposed by a number of models[21,22] and also within the context of fragility.[7] The Adam−Gibbs approach[21] establishes a direct link between viscosity and excess configurational entropy, S_c, of the system; the temperature behavior of the relaxation time is expressed by an exponential relation that contains S_c in the argument. The relaxation expression qualitatively accounts for most of the phenomenology of liquid glass-formers including the strong/fragile liquid pattern.[5] The most recent Di Marzio−Yang model[23] proposes a kinetic theory of glasses where the zero frequency viscosity is mainly determined by the free energy of the system. This approach is based on an equilibrium theory and provides for a connection between specific heat and relaxation behavior over the glass-transition region. Angell and coworkers[7] suggest a correlation based on the energy landscape model that predicts a close link between the temperature evolution of the thermodynamic states of a system and its relaxation properties over the glass-transition region. This means that fragile liquids, when heated through T_g, readily experience transitions over a wide range of configurational states, which drive the corresponding variations in the relaxation times. All models discussed above lead to the prediction that glasses with small specific heat changes at the glass transition exhibit little curvature on $\log \eta$ or $\log \tau$ versus $1/T$ plots, whereas glasses with large specific heat changes are characterized by a significant positive curvature.

At variance with the expectations of the models, accurate examinations of fragility data over a wide range of polymers[8,9] revealed that an increase in the dynamic fragility, m, is paralleled by a decrease in the thermodynamic fragility, evaluated by ΔC_p or $C_{p,l}/C_{p,g}$.

The puzzling aspect concerning polymer fragility also regards HPN. Growing network or cross-link density depresses both the dielectric[3] and mechanical[23] primary relaxations, but gives rise to an enhancement of the dynamic fragility, m. In clear contrast with this observation, the thermodynamic fragility decreases with increasing network density, and a plot of m versus $C_{p,l}/C_{p,g}$ discloses a negative slope (inset of Figure 6). These contrasting evaluations of fragility in HPN surely reflect differences in the coupling between the various experimental probes and the internal degrees of freedom driving the structural rearrangements of large molecular groups. The main question is that, as already emphasized,[8,9] these observations raise doubts about the application of the cited models to polymers. The energy landscape model surely offers a substantial tool for the exploration of the connection existing between transport and thermodynamic properties of glass-forming liquids, but it may be that some important factors determining the mobility of the polymer systems have not been taken into due consideration. A very recent study of light scattering on some polymers[24] reveals that the sensitivity of the fast dynamics to pressure varies in relation to the different temperature regions explored by the system: the volume contribution dominates the fast relaxation behavior in the liquid state, whereas the thermal energy becomes more important in the glassy state. This can imply that polymer could have an energy landscape sensitive to thermal and volume effects, the latter being completely neglected in the models discussed above.

The increase in m with increasing cross-linking in HPNs can be explained by a different vision of the fragility concept, which is more suitable for polymers. In fact, the term "fragility" describes the inability of glass-former liquids to preserve the short- and medium-range order against the thermal degradation. Polymers are not expected to show modifications of the chain structure in the temperature region above T_g, so it is believed[25] that the concept of "cooperativity" better reflects the physical behaviors of these glass-formers. Considering the cooperativity as a measure of the number of molecular units or chain segments that are involved in some kind of collective motion, it is clear that the presence of cross-links increases this number, giving rise to an enhancement of cooperativity in the system. In this context, the growing amount of cross-links in HPN increases the scale of the long-range correlations in the segmental motions within the network and, at the same time, causes a reduction of the configurational degrees of freedom of shorter network chains: the decreasing jumps ΔC_p of the specific heat capacity observed at T_g with increasing network density should be associated with decreasing variations of the configurational entropy. The revealed discrepancies in the fragility behaviors indicate that the description of cooperative relaxations in polymers within the fragility framework needs to be more deeply explored before discussing the relaxation dynamics within a more general context including inorganic glass-forming liquids. Clarification of this question requires extensive wide ranging studies of polymer systems.

Summary

Measurements of dynamic mechanical analysis have been performed to investigate the relaxation dynamics of HPNs over the temperature range below and above T_g, revealing a subglass β-process and the primary α-relaxation. By systematically transforming the basic structural units, the ISHs, from two- to three-arm rings linked by $(CH_2)_6$ bridging groups, it has been shown that growing a connectivity between the molecular units leads to restrictions of the cooperative segmental dynamics. Constraints due to cross-links shift the glass−rubber transition to higher temperatures and reduce the strength of the mechanical α-relaxation, as a clear indication of a growing hindrance experienced by the long-range segmental motion. In clear contrast with this evidence, the behavior of the secondary mechanical β-relaxation with increasing network density reveals a systematic enhancement of the relaxation strength, the local segmental mobility being enhanced by the increasing number of network junctions. The mechanical β-relaxation follows an Arrhenius-like law with increasingly higher frequency factors and activation energies from $\sim 10^{15}$ s^{-1} and 44.2 kJ/mol in linear HPN to $\sim 10^{19}$

s^{-1} and 69.8 kJ/mol in fully cross-linked HPN. Following an analysis proposed by Starkweather, these unusually high values of ω_0 have been discussed in terms of an increasing intermolecular cooperativity of the conformational transitions underlying the β-relaxation arising from the growing inclusion of $(CH_2)_6$ arms bridging between the ISH rings. Also accounting for the marked variation of the thermal expansion observed over the same temperature range of the β-relaxation, the crankshaft motion of the arms, whose correlated moves lead to the significant value of activation entropy characterizing the process in fully cross-linked HPN, has been suggested as its possible origin. Comparison with previous data concerning the dielectric β-relaxation in the same HPNs discloses significant differences that indicate a less cooperative character and a different microscopic origin for the conformational transitions driving the dielectric process.

Finally, the observed decrease in the thermodynamic fragility with increasing cross-linking has been interpreted in terms of a heterocyclic network whose morphology is characterized by decreasing degrees of freedom originating a decrease in the configurational entropy of the system. The decrease in the thermodynamic fragility is paralleled by an increasing dynamic fragility, as measured by dielectric and mechanical spectroscopy. This contrasting behavior for the thermodynamic and dynamic measures of fragility strictly follows the trend already evidenced in a wide class of polymers.

Acknowledgment. We wish to dedicate this article to the memory of Prof. Valery P. Privalko, who inspired this work and provided the samples for the present study. It was a honor and a privilege for us to have known a man of such important achievement and personality, who was always innovative and enthusiastic, open to new ideas, and always willing to share his thoughts with colleagues.

References and Notes

(1) Starkweather, H. W. *Macromolecules* **1981**, *14*, 1277. ibidem **1988**, *21*, 1798; ibidem **1990**, *23*, 328; ibidem **1993**, *26*, 4805.
(2) Matsuoka, S.; Hale, A. *J. Appl. Polym. Sci.* **1997**, *64*, 77.
(3) Kramarenko, V.Yu.; Ezquerra, T. A.; Sics, I.; Balta Calleja, F. J.; Privalko, V. P. *J. Chem. Phys.* **2000**, *113*, 447.
(4) Kramarenko, V.Yu.; Ezquerra, T. A.; Privalko, V. P. *Phys. Rev. E* **2001**, *64*, 051802.
(5) Angell, C. A. *J. Non Crystalline Solids* **1991**, *131−133*, 13. Angell, C. A. *Science* **1995**, *267*, 1924.
(6) Böhmer, R.; Ngai, K. L.; Angell, C. A.; Plazek, D. J. *J. Chem. Phys.* **1993**, *99*, 4201.
(7) Ito, K.; Moynihan, C. T.; Angell, C. A. *Nature* (*London*) **1999**, *398*, 492.
(8) Roland, C. M.; Santangelo, P. G.; Ngai, K. L. *J. Chem. Phys.* **1999**, *111*, 5593.
(9) Huang, D.; McKenna, G. B. *J. Chem. Phys.* **2001**, *114*, 5621.
(10) Robertson, C. G.; Lin, C. J.; Rackaitis, M.; Roland, C. M. *Macromolecules* **2008**, *41*, 2727.
(11) Fischer, E. W.; Hellmann, G. P.; Spiess, H. W.; Hörth, F. J.; Ecarius, U.; Herle, H. *Makromol. Chem. Suppl.* **1985**, *12*, 189.
(12) Boyer, R. F. *Rubber Chem. Technol.* **1963**, *34*, 1303.
(13) Boyd, R. H. *Polymer* **1985**, *26*, 1123.
(14) Schatzki, T. F. *J. Polymer Science-Part C* **1966**, *14*, 139.
(15) Hartwig, G. *Polymer Properties at Room and Cryogenics Temperatures*; Plenum Press, New York, 1994.
(16) Bartolotta, A.; Di Marco, G.; Lanza, M.; Carini, G. *J. Polym. Sci. B: Polym. Phys.* **1995**, *33*, 93.
(17) Di Marco, G.; Bartolotta, A.; Carini, G. *J. App. Phys.* **1992**, *71*, 5834.
(18) Carini, G.; Cutroni, M.; Federico, M.; Tripodo, G. *Phys. Rev. B* **1988**, *37*, 7021.
(19) Berret, J. F.; Meissner, M. *Z. Phys. B-Cond. Matter* **1988**, *70*, 65.
(20) Ferry, J. D. *Viscoelastic properties of polymers*; John Wiley & Sons: New York, 1970.
(21) Kramarenko, V.Yu.; Alig, I.; Privalko, V. P. *J. Macromolecular Science: Part B: Phys.* **2005**, *44*, 647.
(22) Adam, G.; Gibbs, J. H. *J. Chem. Phys.* **1965**, *43*, 139.
(23) Di Marzio, E. A.; Yang, A. J. M. *J. Res. Natl. Inst. Stand. Technol.* **1997**, *102*, 135.
(24) Hong, L.; Begen, B.; Kisliuk, A.; Novikov, V. N.; Sokolov, A. P. *Phys. Rev. B* **2010**, *81*, 104207.
(25) Roland, C. M.; Ngai, K. L. *Macromolecules* **1991**, *24*, 5315.